ISSN1346－7832

独立行政法人港湾空港技術研究所

港湾空港技術研究所報告

REPORT OF THE PORT AND AIRPORT RESEARCH INSTITUTE

VOL.40 NO.3 September 2001

NAGASE, YOKOSUKA, JAPAN

INDEPENDENT ADMINISTRATIVE INSTITUTION,
PORT AND AIRPORT RESEARCH INSTITUTE

港湾空港技術研究所報告 (REPORT OF PARI)

第 40 巻 第 3 号 (Vol.40, No.3), 2001 年 9 月 (September 2001)

目 次 (CONTENTS)

港湾空港技術研究所報告
第40巻第3号(2001.)

海洋環境下におけるＲＣ構造物中の鉄筋腐食に関する長期暴露試験

タレク　ウディン　モハメッド*・濵田　秀則**・山路　徹*

要　旨

コンクリート中の鉄筋の腐食は海洋構造物の耐久性低下の最も大きな原因となっている．この問題に関しては，古くから多くの研究が実施されてきている．しかし，海洋環境下におけるＲＣ構造物の長期耐久性を確保するためには，まだまだ多くの研究が必要である．このために，海洋環境下におけるコンクリート構造物の耐久性に関する重要な幾つかの点に関して長期の暴露試験を実施し，幾つかの結論を導いた．

過去６年間にわたる一連の研究プログラムにおいて，コンクリート中鉄筋の電気化学的性質，物理的性質，例えば，鉄筋の配置方向が腐食に及ぼす影響，異型棒鋼と丸鋼の腐食状況の相違，コンクリートのひび割れが腐食に及ぼす影響，普通セメント・高炉セメント・フライアッシュセメントといったセメントの種類が腐食に及ぼす影響，などについて研究を実施してきた．本文においては，これらの研究より得られた結果を取りまとめ，以下に示す結論を得た．

1)　鉄筋とコンクリートの間に空隙が存在する場合は，腐食発生時期を早めるとともに，一旦腐食が開始された鉄筋の腐食速度が大きくなる．

2)　丸鋼に比べて異型棒鋼の方が腐食しやすい傾向にあった．

3)　高炉スラグ置換率が比較的高い，高炉セメントＣ種が最も塩分浸透に対する抵抗性，内部鉄筋の腐食抵抗性が優れていた．

4)　長期の暴露期間において，比較的幅の小さなひび割れは水和生成物により充填される傾向にあり，そのために内部鉄筋の腐食が抑制される傾向にあった．

キーワード：耐久性，腐食，鉄筋－コンクリート界面，ひび割れ幅，混合セメント，異型棒鋼，丸鋼

*　地盤・構造部　材料研究室　研究官

**　地盤・構造部　材料研究室　室長

〒239-0826　横須賀市長瀬3-1-1　独立行政法人　港湾空港技術研究所

電話：0468-44-5061　Fax：0468-44-0255　　e-mail：tarek@pari.go.jp

TECHNICAL REPORT OF THE PORT AND
AIRPORT RESEARCH INSTITUTE
Vol. 40., No. 3, 2001.

Corrosion of Steel Bars in RC Structures Under Marine Environment Based on the Long-Term Exposure Tests

Tarek Uddin MOHAMMED*

Hidenori HAMADA**

Toru YAMAJI***

Synopsis

Corrosion of steel bars in concrete is a major cause of deterioration of reinforced concrete structures exposed to the marine environment that leaded to a loss of multi-billion US$ every year. A lot of researches were executed on this matter since long ago. However, studies on this matter are still necessary in order to ensure long-term durability of marine RC structures. With this aim, several conclusions are drawn here based on the investigations on several research topics regarding the durability of concrete structures under marine environment.

Detail electrochemical as well as physical evaluations of steel bars corrosion were carried out on several experimental programs in the last six years, such as corrosion of steel bars with respect to its orientation in concrete, corrosion of plain and deformed steel bars in concrete, corrosion of steel bars in cracked and uncracked concrete made with ordinary, fly ash and slag cements. The summaries of these investigations are reported here with the following conclusions:

- Voids/gaps at the steel-concrete interface cause earlier corrosion and accelerate the rate of corrosion of steel bars in concrete,
- Deformed bar is more prone to corrosion compared to plain bar,
- Slag cements with higher amount of slag content, such as Slag Cement of Type C shows the best performance against chloride ingress and corrosion of steel bars in concrete,
- With the continued exposure under marine environment, narrow cracks are healed and stopped the corrosion process.

Key Words: blended cements, corrosion, crack width, deformed bar, durability, plain bar, steel-concrete interface.

* Research Engineer of Materials Division, Geotechnical and Structural Engineering Department

** Chief Research Engineer of Materials Division, Geotechnical and Structural Engineering Department

*** Research Engineer of Materials Division, Geotechnical and Structural Engineering Department

3-1-1 Nagase, Yokosuka, 239-0826 Japan.

Phone : +81-468-44-5061 Fax : +81-468-44-0255 e-mail : tarek@cc.phri.go.jp

Contents

1. Introduction

Concrete as the most commonly used construction material is recognized worldwide since long ago. About two tons of concrete is placed per capita of the world population every year. Based on the estimation of the world population at 6 billion, it can be judged that every year about 12 billion tons of concrete is placed. Form the viewpoint of accumulated maintenance and repair works of the existed and newly constructed concrete structures, it is easily realized that a huge pressure is coming to the concrete professionals. On the other hand, it is also realized that the design of a long-term durable concrete structure will reduce the cement consumption, which will result the reduction of carbon dioxide emission to the global atmosphere. About one ton of carbon dioxide is emitted to the global atmosphere per ton of cement production [1]. Even though the total amount of carbon dioxide emission (about 7% of total carbon dioxide emission in the world) from the cement producing industries is much lower compared to the other sources of carbon dioxide emissions, such as thermal power plants, vehicles etc. However, it will give a positive impact to the global atmosphere. With this background, the importance of making long-term durable concrete structure is realized. Several international conferences are organized by ACI and CANMET in the last few years with the goal of the achievement of sustainable development of concrete technology. There are many reasons of earlier deterioration of concrete structures. Among them, deterioration of concrete structures due to the corrosion of steel bars in concrete is a common matter. The authors carried out several experimental investigations in order to understand the process of earlier initiation of corrosion of steel bars in RC structures. Both accelerated short-term and long-term exposure tests were carried out. The long-term exposure tests were carried out in the tidal pool of *Port and Airport Research Institute, Independent Administrative Institution, Yokosuka, Japan*. In this paper, the main results of the previous investigations are summarized in separate sections with a short background and experimental procedure. The results will be very useful to enhance long-term durability of marine concrete structures. Further details of each of the investigations can be obtained in the relevant references noted in this report.

2. Corrosion of Steel Bars Due to the Voids/Gaps at the Steel Concrete Interface

The presence of voids/gaps around the steel bars may lead to the earlier corrosion of steel bars. A few studies were focused on this matter. In order to enhance long-term durability of RC structures in the marine environment, this matter should be seriously considered. In this section, the process of corrosion with the presence of voids is summarized. Further detail of these investigations can be obtained in **References 2, 3, and 4.**

2.1 Experimental Procedure

The detailed experimental setup is shown in **Fig. 2.1.** Mix proportions of concrete relevant to the results reported here are listed in **Table 2.1.** OPC was used in this investigation. Natural river sand and crushed granite were used as aggregates. In each specimen, one stirrup and four main steel bars were embedded. The diameter of stirrup and main steel bars was 13 mm. The stirrup was specially fabricated with several steel segments, such as HTT, HTB, BT, VT, VM, VB, HBB, HBT and BB. Main Steel elements were TM and BM. The detail explanations of these symbols are noted in **Fig. 2.1.** All steel elements were connected with epoxy to isolate them from direct electrical connection inside the specimen. The steel elements were electrically connected at the outside of the specimen through electric wires. Fourteen electrical joints were provided in each specimen. This complicated layout of the specimen was planned in order to measure the flow of the macro-cell corrosion currents through all of the steel elements and also to measure the polarization resistance of the steel elements separately without any interaction from the other steel elements. Specimens were also made without dividing the stirrups. In order to accelerate the corrosion process, NaCl as 10 kg/m^3 of concrete was added with the mixing water. Macro-cell and micro-cell corrosions of the steel elements were measured periodically. After electrochemical investigations, the specimens were cut across the steel bars and steel-concrete interfaces were checked with an optical microscope. The specimens were also broken open to visualize the condition of the steel bars and also to measure the corroded area over the steel elements.

2.2 Macro-cell and Micro-cell Corrosions

Macro-cell corrosion current densities of the steel elements are shown in **Fig. 2.2.** HTB, HBB and TM steel elements are anode, and other steel elements are cathode. The anodic (dissolution of iron) and cathodic (consumption of electrons) areas are involved with the following reactions over the steel surface:

$$Fe \rightarrow Fe^{++} + 2e$$

$$\frac{1}{2}O_2 + 2H_2O + 2e \rightarrow 2(OH)^-$$

The cathodic areas are coupled with the anodic areas in order to consume the electrons generated at the anodic areas. HTB steel element, i.e., the bottom half of the top-level horizontal steel bars, and TM steel element are subjected to significant macro-cell corrosion. This is attributed to the formation of gaps under these elements, which is explained later.

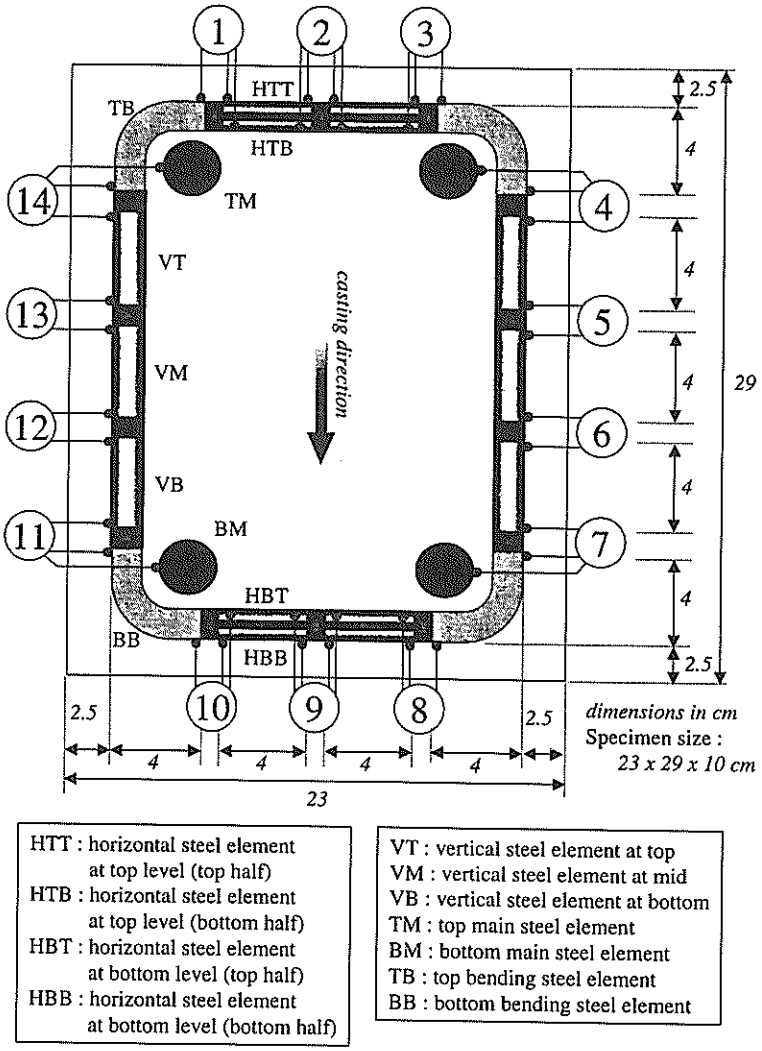

Fig. 2.1 Layout of the Specimen

Table 2.1 Mix Proportions

G_{max} , mm	20
Slump, cm	15±3
Air, %	5±1
W/C, %	50
s/a, %	45
W, kg/m^3	165
C, kg/m^3	330
S, kg/m^3	803
G, kg/m^3	988
*P-70, ml/m^3	760
**N-303, ml/m^3	13.2

*P-70 is a water-reducing admixture

**N-303 is an air-entraining admixture.

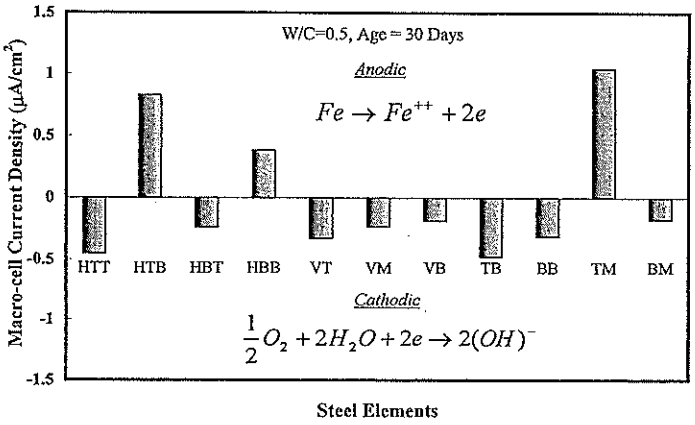

Fig. 2.2 Macro-cell Corrosion

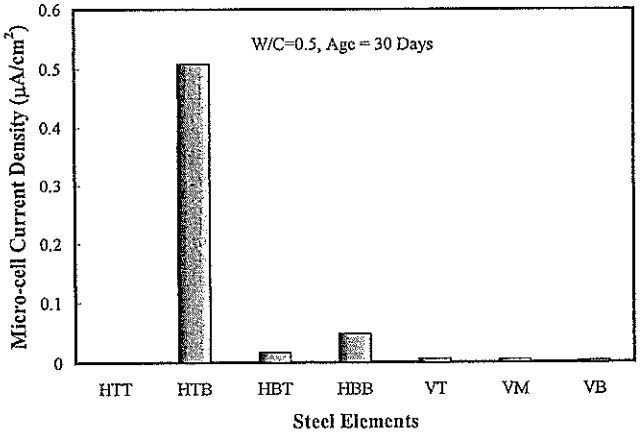

Fig. 2.3 Micro-cell Corrosion

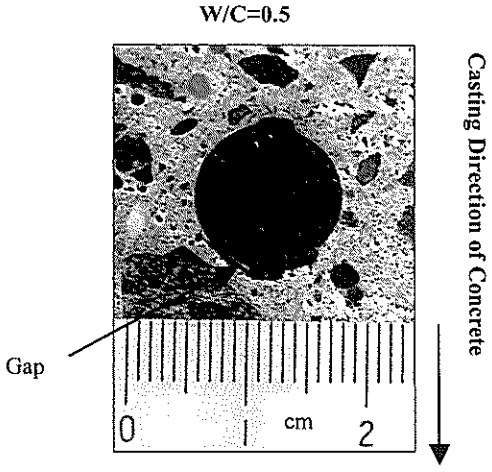

Fig. 2.4 Gaps Under the Steel Bars

Micro-cell current densities of the steel-elements are shown in **Fig. 2.3.** Comparatively higher micro-cell corrosion is observed over HTB steel element. Micro-cell corrosion current densities of the vertical (casting direction of concrete was along the steel elements) and other steel elements are very low.

The presence of gap/void under the horizontal steel bar is shown in **Fig. 2.4,** which causes the above-mentioned results. The gap under the horizontal steel elements creates due to the plastic settlement of concrete as well as blocking of bleeding water under the horizontal steel bars after casting concrete. The steel-concrete interfaces of the vertical steel elements (VT, VM and VB) were checked and no voids were found surrounding the steel bars. Also the same situation was observed over HTT and HBT steel elements.

More detail results of this investigation can be obtained in **Reference 2.**

2.3 Visual Observation

Corroded area of the steel elements are listed in **Table 2.2** qualitatively. HTB steel element corrodes significantly, however, almost no corrosion is observed

over HTT, HBT, VT, VM, VB elements. A little trace of corrosion is also observed over HBB and under TB elements. Trace of corrosion is also observed over the bottom halves of TM steel elements.

Table 2.2 Corroded Area over the Steel Elements

Element	Corroded Area
HTT	No corrosion
HTB	Totally corroded
HBT	No corrosion
HBB	Few spots
VT	No corrosion
VM	No corrosion
VB	No corrosion
TB	Few spots
BB	No corrosion
TM	Bottom half totally corroded
BM	Few Spots at the bottom half

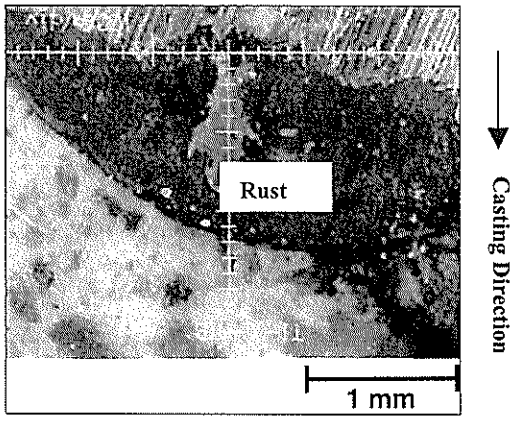

Fig. 2.5 Steel-Concrete Interface (After 23-Year of Exposure)

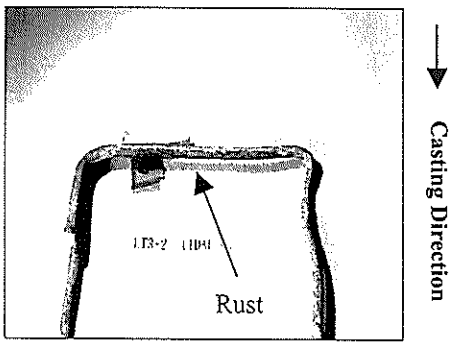

Fig. 2.6 Condition of the Stirrup (After 23-Years of Exposure)

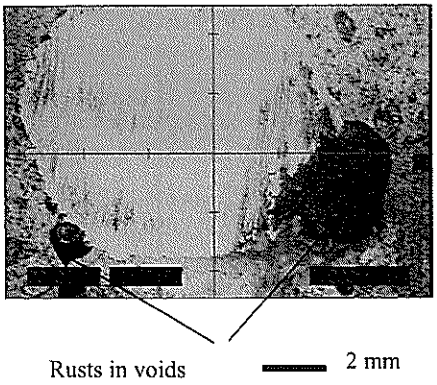

Fig. 2.7 Condition of the Steel Bar (After 15 Years of Exposure)

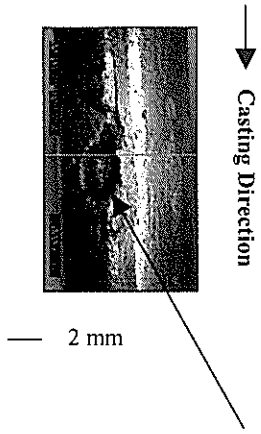

Fig. 2.8 Condition of the Steel Elements (After 15 Years of Exposure)

2.4 Further Accelerated Exposure Investigation

In the above-mentioned experiment, sodium chloride as 10 kg/m^3 was added with the mixing water during mixing concrete. The reason was to accelerate the process of corrosion. However, generally chloride ion diffuses into concrete from the outside environment. Therefore, a question can be raised about the validity of the above-mentioned accelerated experimental condition. In order to verify this, more investigations were carried out allowing chloride ion penetration from the outside environment. Same process of corrosion was obtained as before. The detail of this investigation is reported in **Reference 5.** Furthermore, the process of corrosion was also verified with the long-term exposure tests. These results are explained in the following section.

2.5 Long-term Exposure Tests

In order to verify the above-mentioned accelerated tests, several investigations were carried out utilizing

23-year and 15-year old reinforced concrete specimens. The detail results of these investigations are reported in **References 3 and 4**. The observation of the steel-concrete interface with respect to the casting direction of concrete is shown in **Fig. 2.5**. The amount of water soluble chloride ion concentration over the steel bars was about 1% of cement weight. After 23 years of exposure, the bottom parts of the horizontal steel bars corroded significantly. It is attributed to the presence of gap under the horizontal steel bars as before. This location is the same as the HTB steel elements as explained before. The top portion of the steel bars (same as HTT) was not corroded even though chloride ions reach at this location first. This is due to its better interface with concrete. The vertical legs of the stirrups were also not corroded (same as VT, VM and VB) due to its better interface with concrete. A typical case is shown in **Fig. 2.6**. Water soluble chloride ion concentration around the stirrup was more than 1% of cement weight. This value was much higher than the chloride threshold limit against the initiation of corrosion [6]. Therefore, it is understood that the chloride threshold values can be increased to a higher level, if the steel-concrete interface is free from gap/void.

The steel-concrete interface of 15-years old specimens exposed to the tidal environment is shown in **Fig. 2.7**. Detail of these specimens is reported in **Section 5**. The presence of corrosion pits is found at the locations having voids at the steel-concrete interface.

The condition of the steel bars of 15 years old concrete specimens (exposed to tidal environment) is shown in **Fig. 2.8**. The detail of the specimens is reported in **Section 4**. Here, casting direction of concrete was along the steel bars. Due to the inappropriate compaction, voids are formed at the steel-concrete interface. This leads to the formation of localized pit even for casting direction of concrete along the steel bars.

2.6 Summary

The importance of making concrete without gaps/voids at the steel-concrete interface can be realized from these investigations. The presence of voids/gaps causes the earlier initiation of corrosion. The area of the steel surface with voids/gaps acts as anode and coupled with the other regions to form a macro corrosion cell. Also, the areas with gap/void subjected to significant amount of micro-cell corrosion locally.

It is concluded that making concrete without voids or gaps at the steel-concrete interface is very essential in order to enhance long-term durability of RC structures in the marine environment.

3. Corrosion of Plain and Deformed Bars

Deformed bars are commonly used for its good bonding strength compared to plain bars. However, no detail study was performed in order to compare corrosion rate of plain and deformed bars in concrete. The authors carried out several experimental investigations in order to compare the corrosion rate of plain and deformed bars in concrete. The detail of these investigations can be obtained in **References 7 and 8**.

3.1 Experimental Procedure

The layout of the specimens is shown in **Fig. 3.1**. Cracking and anchoring process of the beams are also shown in the same figure. RC beams were made with plain and deformed bars separately. They were cracked with the same load at the laboratory. Crack widths were recorded at the maximum load. Then the beams were anchored in pair and tried to maintain the crack widths as before. Mix proportions of concrete relevant to the data reported here are listed in **Table 3.1**. Chemical compositions of the steel bars are shown in **Table 3.2**. The compositions satisfied the limits provided by JIS. The beams were exposed under the open sky. To accelerate corrosion process, 3.5% salt water was sprayed once a week over the specimens. Electrochemical investigations on the specimens were carried out periodically. After electrochemical investigations, chloride ions in concrete were measured. Finally, the specimens were broken open to see the condition of the steel bars.

3.2 Polarization Resistance, Concrete Resistance and Chloride Ion Concentrations

Polarization resistance and concrete resistance data over the cracked concrete beams are shown in **Fig. 3.2**. In the same figure, crack faces of the beams are also shown. More number of cracks is observed over the beams reinforced with deformed bars compared to the same with plain bars. However, the crack widths are narrower in the case of the beam reinforced with deformed bars. These will not cause more corrosion over plain bars as noted later.

Lower polarization resistance and lower concrete resistance over the deformed bars are clearly observed. The rate of corrosion is calculated from the following equation [9]:

$$I = \frac{B}{R_p}$$

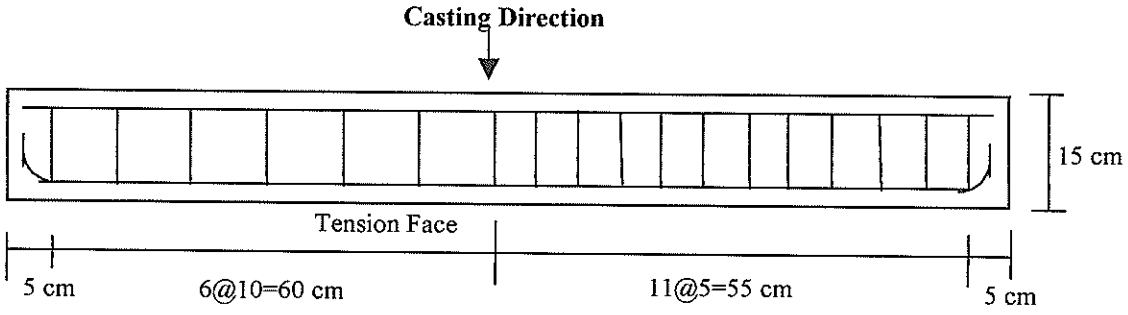

Longitudinal Section

Specimen

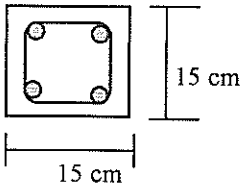

Diameter of the stirrup = 6 mm
Diameter of the main bar = 13 mm
Concrete cover = 25 mm

Transverse Section

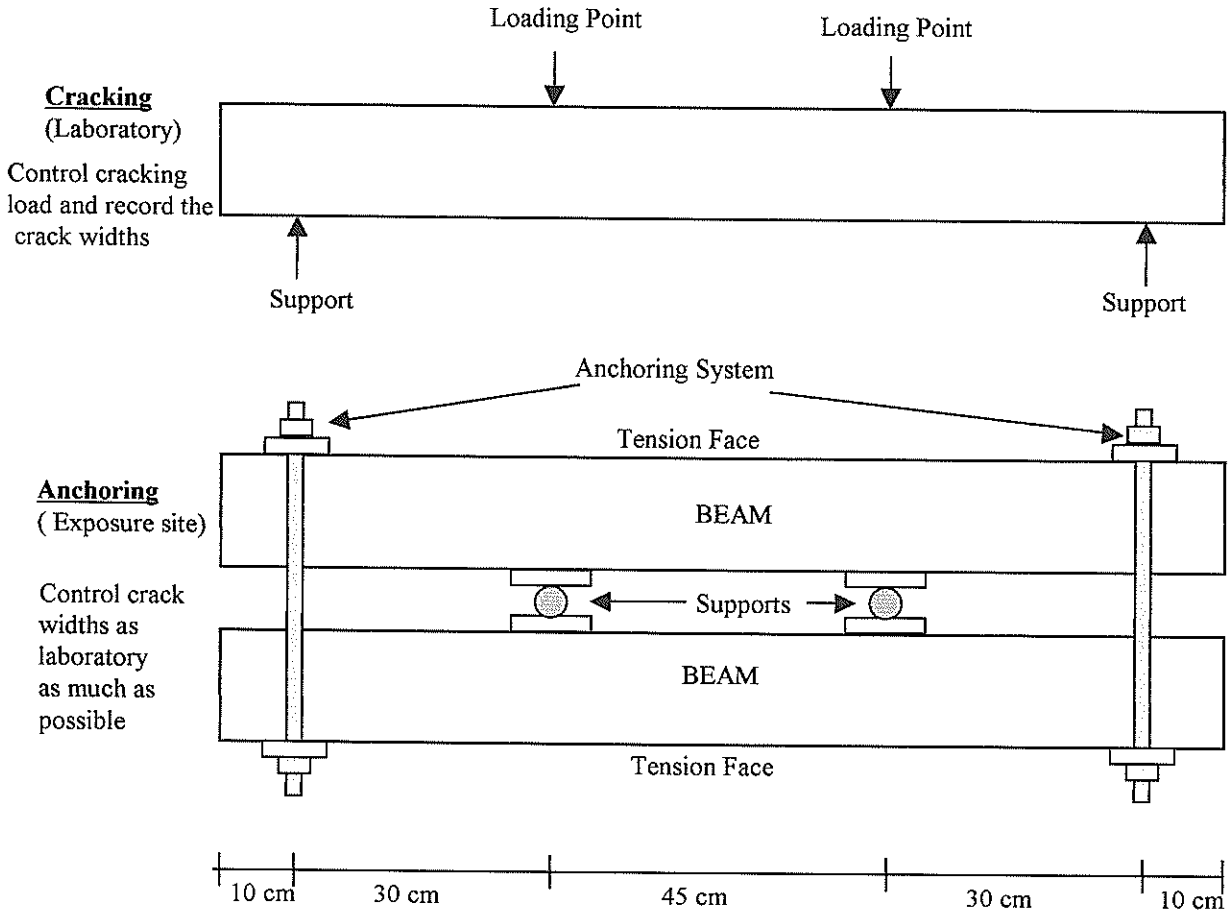

Fig. 3.1 Detail Layout of the Specimens

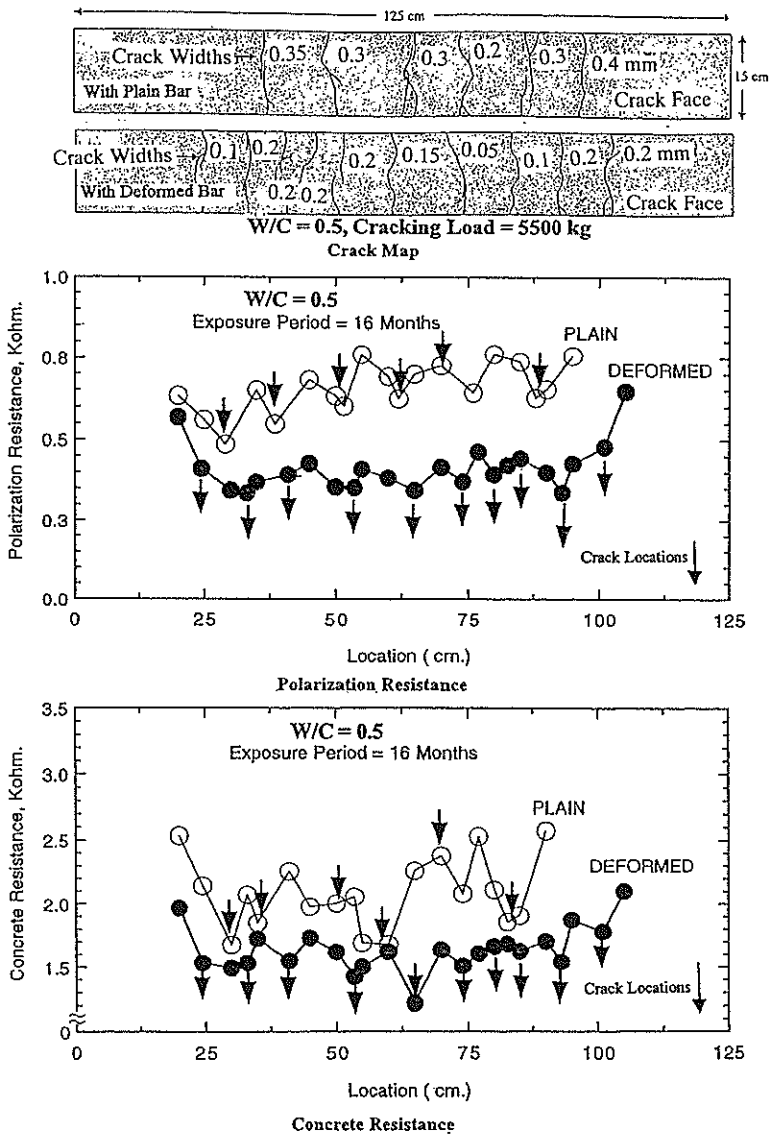

Fig. 3.2 Crack Face of the Beam with the Distribution of Polarization Resistance, Concrete Resistance along the Beam

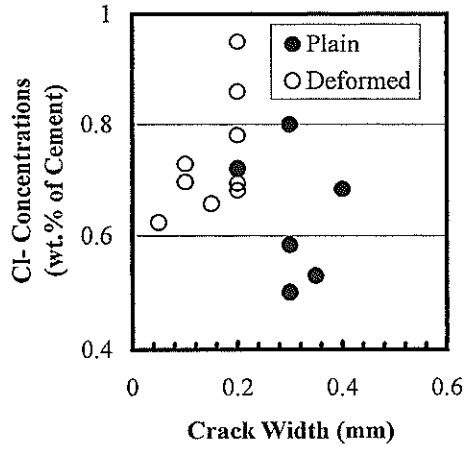

Fig. 3.3 Chloride Ion Concentrations at the cracked regions

Table 3.1 Mix Proportions

G_{max} , mm	20	20
Slump, cm	*8 ± 2*	*8 ± 2*
Air, %	5±1	*5 ± 1*
w/c, %	50	70
s/a, %	45	45
W, kg/m^3	165	165
C, kg/m^3	330	236
S, kg/m^3	803	837
G, kg/m^3	988	1031
P-70, ml/m^3	760	637
N-303, ml/m^3	13.2	9.5

Table 3.2 Chemical Compositions of the Steel Bars

	C	Si	Mn	P	S
Def.	0.22	0.16	0.76	0.025	0.031
Plain	0.17	0.27	0.72	0.024	0.012

All in %.

Here, I is the micro-cell corrosion current density, B is a constant. An average value of B is considered as 0.026 V [9,10]. From the above equation, higher corrosion rate can be judged for lower polarization resistance data. Therefore, the micro-cell corrosion rate over the deformed bars will be higher than the plain bars. Based on this experimental setup, macro-cell corrosion cannot be evaluated. In another series of specimens with a different experimental setup, macro-cell current densities were measured. It was found that macro-cell corrosion current density over the deformed bars was higher than the same over the plain bars. The results were reported in **Reference 8.**

After depassivation of the steel bars, it is the cathodic reaction, which controls the rate of corrosion. The movements of the ions in concrete with low concrete resistance will be faster and will accelerate the rate of cathodic reaction. Therefore, the lower concrete resistance over the deformed bars will lead to increase the rate of corrosion. Water soluble chloride ion concentrations over the steel bars at the cracked regions are shown in **Fig. 3.3**. Chloride ion concentration over the deformed bars was higher than the same over the plain bars. It also will cause to increase the rate of corrosion over deformed bars.

The above-mentioned results indicate the higher corrosion rate over the deformed bars compared to the plain bars. The reason can be explained due to the severe micro-cracking in concrete reinforced with deformed bars. Generally, micro-cracking as well as crack numbers of the beam with deformed bar is higher than the same with plain bars [11]. In a recent study, it was also concluded that the crack frequency is the most influential factor rather than the crack width [12]. The beams with plain bars have lower number of cracks compared to the same with deformed bars. Due to the severe micro-cracking and more numbers of crack, the quality of concrete with deformed bars will reduce significantly. It consequences more corrosion rate over deformed bars.

W/C=0.7, Age of Exposure = 16 Months

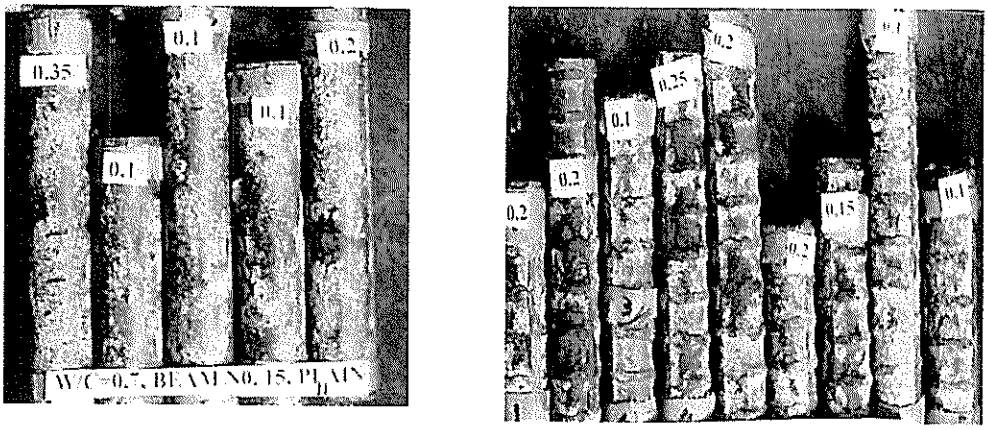

Taken from a beam with plain bar Taken from a beam with deformed bar

Fig. 3.4 Condition of the Steel Segments at the Cracks

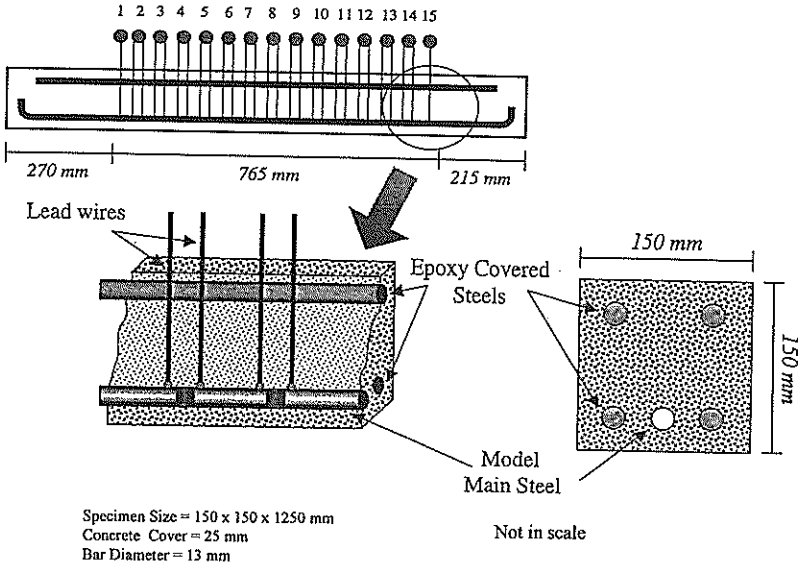

Fig. 3.5 Experimental Setup of Oxygen Permeability Measurement

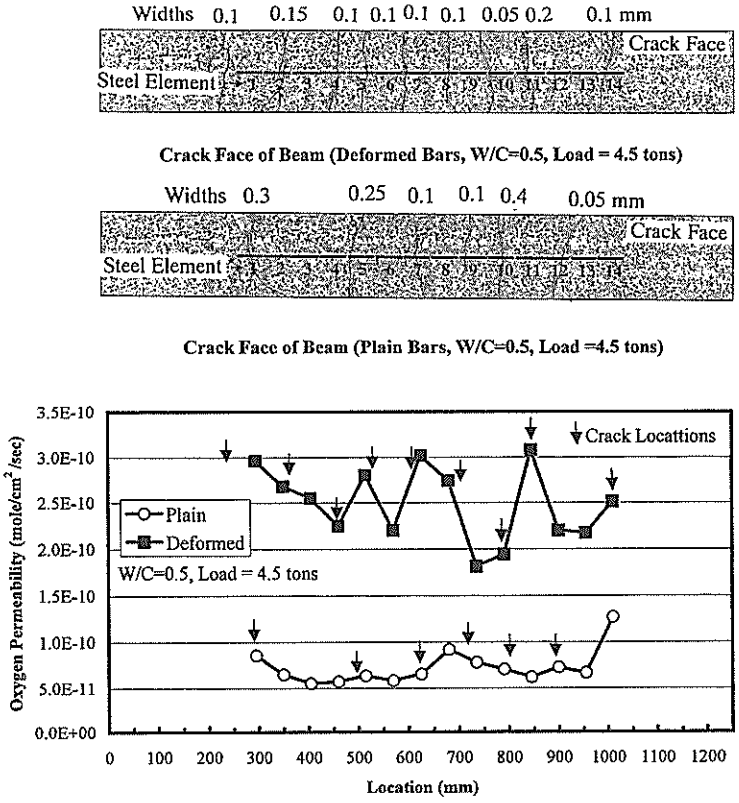

Fig. 3.6 Crack Face of the Beam with the Distribution of Oxygen Permeability

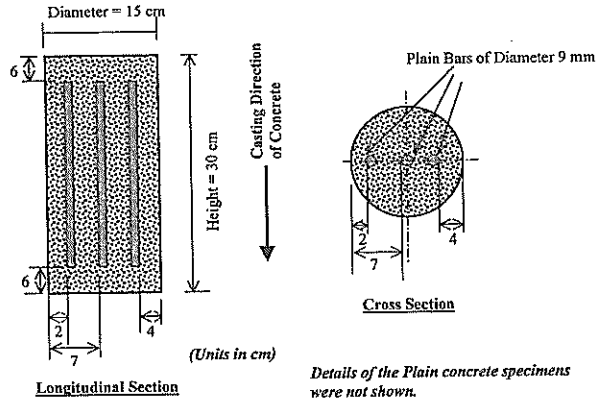

Fig. 4.1 Details of the Specimen

Table 4.1 Mix Proportions

	OPC	SCA	SCB	SCC	FACB
Gmax(mm)	20	20	20	20	20
Slump(cm)	8±1	8±1	8±1	8±1	8±1
Air (%)	4±1	4±1	4±1	4±1	4±1
W/C (%)	45	45	45	45	45
s/a (%)	41	42	41	41	41
W(kg/m^3)	162	160	160	162	160
C (kg/m^3)	360	356	355	360	356
S (kg/m^3)	738	756	736	714	733
G(kg/m^3)	1110	1091	1108	1120	1103
AEWRA (kg/m^3)	3.60	3.56	3.55	3.60	3.56
AEA (ml/m^3)	360	356	355	360	356

AEA and AEWRA mean air-entraining, and air-entraining water-reducing admixtures.

3.3 Visual Observations

The steel segments at the cracked regions are shown in **Fig. 3.4.** It is observed that deformed bars corroded more than the plain bars. Corrosion of steel bars with respect to crack widths is not explained here as the matter is considered to be out of the scope of this paper. The detail explanation on this matter can be obtained in **Reference 8.**

3.4 Investigation on Oxygen Permeability

Further investigation on the oxygen permeability in cracked concrete with plain and deformed bars was carried out. The detail of the experimental setup is shown in **Fig. 3.5.** A specially fabricated steel bar was embedded in concrete in order to evaluate the oxygen permeability of concrete along the length of the beam. A titanium anode mesh was embedded near the surface of concrete. The beams were cracked with the same load and anchored as before. With the anchoring condition, oxygen permeability in concrete was measured. The results are shown in **Fig. 3.6.** It is clearly observed that the beams with deformed bars show oxygen permeability about five times higher than the same with plain bars. Generally the corrosion rate controlling reaction of steel bar in concrete is the cathodic reaction. More oxygen permeability will result higher rate of corrosion over the deformed bars compared to the plain bars.

3.5 Summary

From the investigations explained in this section, it is understood that a cracked beam reinforced with deformed bars has higher oxygen permeability through concrete, lower concrete resistance over the steel bars, lower polarization resistance over the steel bars, and also higher chloride ion ingress in concrete. Also, the micro-cracking and the crack frequencies are higher for the beam reinforced with deformed bars. These results lead to the faster corrosion rate over deformed bars compared to plain bars.

Therefore, in order to enhance long-term durability, the use of plain bars can be recommended as a reinforcing bar in the design of marine RC structures, if the bonding requirement is satisfied.

4. Corrosion of Steel Bars in Un-cracked Concrete With Different Cements

Microstructures of concrete improved significantly due to the use of blended cements. Many studies were carried out on the corrosion performance of steel bars in concrete made with blended cements. The authors also carried out a detail investigation on the performance of different types of cement utilizing 15-year old reinforced concrete specimens exposed to the tidal environment. The detail results of this investigation were reported in **Reference 4.**

4.1 Experimental Procedure

The layout of the specimens is shown in **Fig. 4.1.** The mixture proportions of the specimens are noted in **Table 4.1.** In each specimen, three steel bars of diameter 9 mm were embedded at the cover depths of 2, 4, and 7 cm. Cement types were Ordinary Portland Cement (OPC), Slag Cement of Type A (SCA), Slag Cement of Type B (SCB), Slag Cement of Type C (SCC) and Fly Ash Cement of Type B (FACB). The definition of these cements can be obtained in JIS R5211-1992 and JIS R5213-1992. After electrochemical investigations, the specimens were broken open to collect the steel bars. Corroded areas and pit sizes were measured. Some specimens were utilized to measure chloride ion concentrations in concrete.

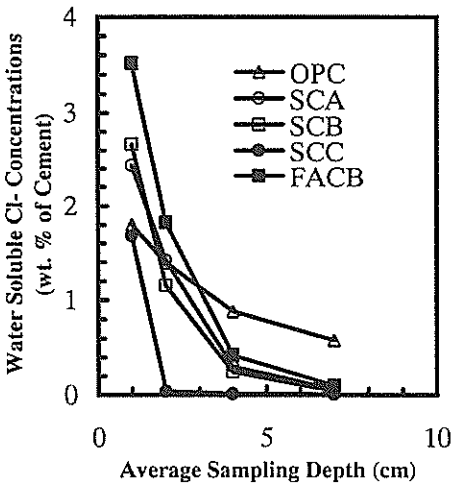

Fig. 4.2 Water Soluble Chloride Ion Concentrations in Concrete

Table 4.2 Diffusion Co-efficient of Chloride Ion

Specimen	Diffusion-Coefficients (mm^2/year)
OPC	75
SCA	16
SCB	12
SCC	8
FACB	15

The compressive strengths of concrete made with OPC, SCA, SCB, SCC and FACB were 37.5, 38.1, 33.5, 29.5 and 46.0 MPa, respectively at the 28 days and 45.7, 41.9, 41.4, 37.1 and 37.0 MPa after 15 years of exposure.

4.2 Chloride Ion Diffusion in Concrete

Water soluble chloride ion concentrations in concrete are shown in **Fig. 4.2.** It is found that in the case of slag cements (especially SCC), chloride ion concentration is concentrated at the surface of concrete. A little amount of chloride ion infiltrates into the inner region of the specimens, especially for concrete made with SCC. It eventually will lengthen the onset of corrosion of the steel bars in concrete made with SCC.

Fick's Second Law of diffusion is commonly used to predict the diffusion of chloride ions in concrete. The closed form solution is expressed below [13]:

$$C(x,t) = C_o\left(1 - erf\left[\frac{x}{2\sqrt{D_{ac}t}}\right]\right)$$

Where, $C(x,t)$ is the chloride ion concentration at a depth x (mm) and time t (year), C_o is the chloride ion concentration at the surface (here it is assumed to be equal to the chloride ion concentration at a mean sampling depth of 1 cm) as weight percentage of cement, D_{ac} is the apparent diffusion co-efficient in mm^2/year, and *erf* is the standard error function. The estimated diffusion co-efficient data based on the chloride ion profiles are summarized in **Table 4.2.** Based on these data, chloride diffusion in concrete is sequenced as OPC>FACB>SCA>SCB>SCC.

Table 4.3 Time to Initiate Corrosion

Specimen	Time to Initiate Corrosion (Year)		
	2 cm	4 cm	7 cm
OPC	2	7	22
SCA	6	26	79
SCB	8	32	98
SCC	12	49	150
FACB	5	21	65

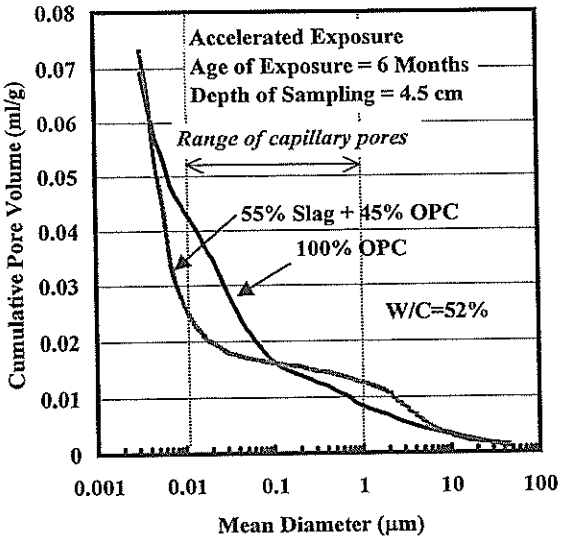

Fig. 4.3 Porosity of Concrete With OPC and Slag Cement

Table 4.4 Micro-cell Corrosions

Specimen	Micro-cell Corrosion Current Density ($\mu A/cm^2$)		
	2 cm	4 cm	7 cm
OPC	0.72	0.25	0.11
SCA	0.56	0.17	0.09
SCB	0.14	0.07	0.05
SCC	0.17	0.05	0.10
FACB	0.51	-	0.07

- Missing Data

Table 4.5 Corroded Area

	Corroded Area (cm^2)		
	2 cm	4 cm	7 cm
OPC	11.82	1.37	0.0
SCA	10.35	0.0	0.0
SCB	0.51	0.0	0.0
SCC	0.0	0.0	0.00
FACB	24.89	0	0.0

Total area of the bars is 45.2 cm^2.

Table 4.6 Number of Pits and Maximum Pit Depths

Specimen	Number of Pits and Maximum Pit Depths (mm)*		
	2 cm	4 cm	7 cm
OPC	6 (1.5)	2 (1)	0 (0)
SCA	3 (1)	0 (0)	0 (0)
SCB	0(0)	0(0)	0(0)
SCC	0(0)	0(0)	0(0)
FACB	5(0.5)	0(0)	0(0)

*The figures in the bracket indicate maximum pit depths. Pit depths higher than 0.5 mm are only counted.
Length of the bar is 16 cm.

Based on the estimated chloride diffusion co-efficient, the time to initiate corrosion of steel bar in concrete with different cements was estimated. The results are listed in **Table 4.3.** For a design concrete cover of 7 cm, the time to initiate corrosion for OPC, SCA, SCB, SCC and FACB are 22, 79, 98, 150 and 65 years, respectively. It clearly confirms the advantage of utilization of slag cements with high slag content (SCB and SCC) to enhance long-term durability of concrete structures in the marine environment

The reason of lower diffusion co-efficient can be explained due to the reduction in capillary pore volume with the utilization of slag cements. In this concern, the porosity results of another investigation with slag cements are reported in **Fig. 4.3**. The reduction in capillary pore volume is observed with the utilization of slag cement.

4.3 Micro-cell Corrosion

Micro-cell corrosion current densities of the steel bars located at the different cover depths are listed in **Table 4.4**. Lower corrosion current density is observed at the higher cover depth. Also, the lower corrosion current density is observed for slag cements, especially for SCC. The reason can be explained due to the lower concentration of chloride ions surrounding the steel bars.

4.4 Physical Evaluations

Corroded areas, number of pits and maximum pit depths are listed in **Tables 4.5 and 4.6**. Less corroded areas and shallower pit depths were observed over the steel bars embedded in the concrete with slag cements.

4.5 Summary

From the results explained in this section, it is clearly understood that utilization of slag cement is necessary to enhance long-term durability of concrete structures in the marine environment. The advantage is more prominent for the cement with higher slag content. It is important to note that a huge amount of slag is produced during the steel-making process and the disposal of this by-product is becoming a critical issue. Annual production of slag throughout the world was estimated at 110 million tons in 1988 and only 30% of it was utilized [14]. More utilization of this cement will also reduce the amount of cement consumption and eventually will reduce the carbon dioxide emission to the global atmosphere. Therefore, utilization of slag cements with a higher amount of slag content (SCC or SCB) will not only enhance the long-term durability of concrete structures but also solve/reduce the global warming and disposal problem of this by-product. Further results on the corrosion of steel bars in cracked concrete with different cements are reported in **Section 5**.

Table 5.1 Chloride Ion Concentrations at the Cracked and Un-cracked Regions

Specimen	Crack Widths (mm) and Water Soluble Chloride Ion Concentrations (Wt. % of C) *		
	1	2	3
OPC	0.2 (1.28) ((1.27))	0.1 (1.14) ((0.64))	0.1 (1.38) ((1.41))
SCA	0.1 (0.33) ((0.17))	0.3 (0.78) ((0.23))	0.2 (0.49) ((0.43))
SCB	0.3 (0.45) ((0.31))	0.1 (0.41) ((0.28))	5 (3.2) ((0.16))
SCC	1.5 (1.67) ((0.19))	0.1 (0.37) ((0.23))	2 (1.84) ((0.69))
FACB	0.1 (0.9) ((0.67))	0.3 (0.82) ((0.29))	0.5 (1.42) ((0.27))

*The figures in (.) and ((.)) indicate chloride ion concentration at cracked and un-cracked regions respectively. The figures without bracket indicate crack widths.

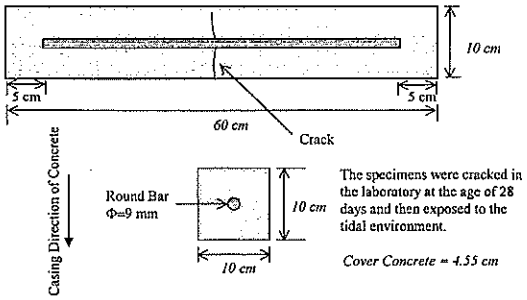

Fig. 5.1 Details of the Specimens

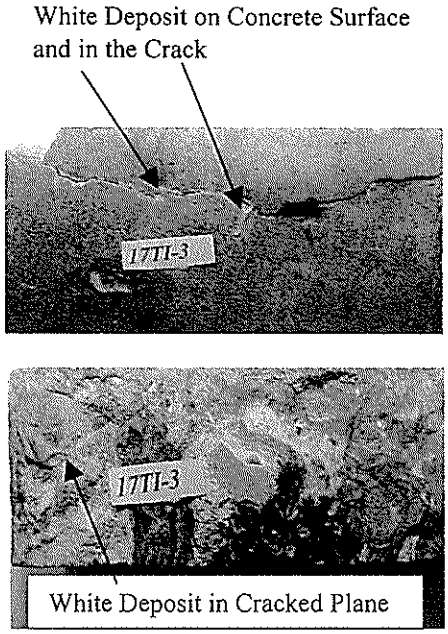

Photographs of Concrete Surface (top) and Cracked plane (bottom). Crack width at the surface is 0.5 mm.

Fig. 5.2 Photographs of the Healed Crack (FACB)

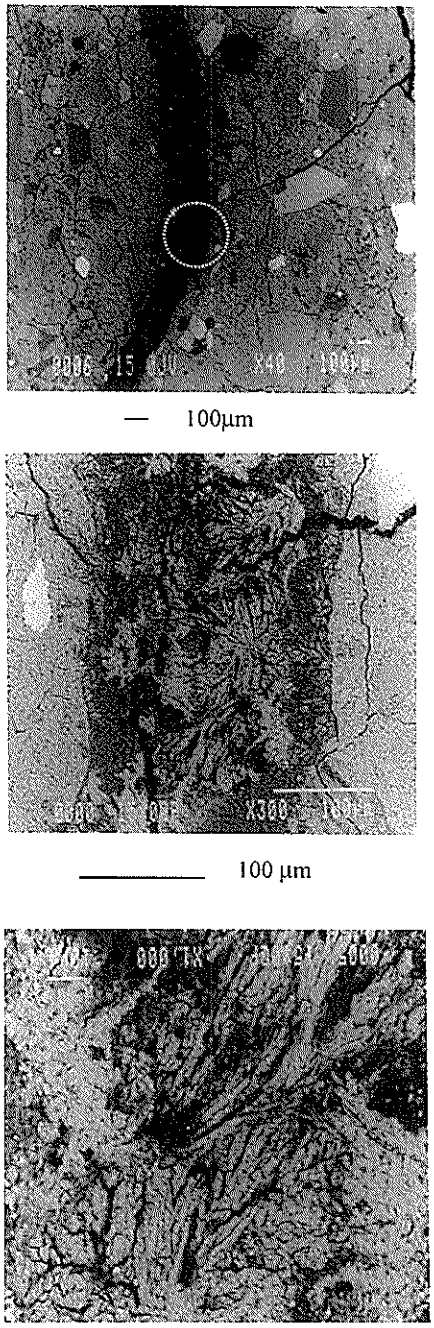

Crack width at the surface = 0.1 mm. Sliced plane is located at 1.3 cm from the surface.

Fig. 5.3 SEM Photographs of the Healed Crack (SCB)

5. Corrosion of Steel Bars in Cracked Concrete Made with Different Cements

In the previous section, corrosion of steel bars in un-cracked concrete with different cements is explained. With the same background of the previous section, in this section, corrosion of steel bars in cracked concrete specimens made with OPC, SCA, SCB, SCC and FACB is noted. Same as the uncracked specimens, the cracked specimens were exposed in the tidal environment for 15 years. The further detail of this investigation is reported in **Reference 15.**

5.1 Experimental Procedure

The detailed layout of the specimen is shown in **Fig. 5.1.** Mix proportions were same as the uncracked specimens reported in **Section 4.** A steel bar was embedded at the center of the specimen. After cracking at the laboratory with a specified width, the specimens

were exposed in a tidal pool for a period of 15 years. Electrochemical investigations were carried out after 15 years of exposure. Chloride ions in concrete at the cracked and un-cracked regions were also measured. Physical evaluations on the corrosion of steel bars were carried out after electrochemical investigations

5.2 Chloride Ion Concentrations

Chloride ion concentrations at the cracked and un-cracked regions are listed in **Table 5.1**. Less amount of chloride ion concentration is observed at the un-cracked region. In the case of wider cracks, significant amount of chloride ion concentration is observed at the cracked region. For narrower crack widths, the chloride ingress into concrete is sequenced as OPC>FACB>SCA>SCB>SCC.

5.3 Healing of the Crack

Narrower cracks (0.5 mm) were healed due to the autogeneous healing. **Figure 5.2** shows the photographs of a healed crack of crack width 0.5 mm on the concrete surface. Deposit is observed even on the surface of the specimens. Clear white deposit is also observed at the crack. EPMA analysis of concrete samples at the cracked regions was also carried out to determine the chemical composition of the deposit. It was found that the deposit composed of calcite, brucite and ettringite. SEM photographs across the cracked region are shown in **Fig. 5.3**. The needle-shaped ettringite can be found from this photograph, which is mixed with other deposits such as calcite and brucite. Crack healing was observed irrespective of the cement types due to the reaction of hydration products of concrete with seawater. The progress of healing with the variation of the cement types cannot be judged from this investigation. However, in another study, it was concluded that the type of cements has no influence on the autogenous healing [16].

5.4 Physical Evaluations

The maximum pit depths of the steel bars at the cracked and un-cracked regions are listed in **Table 5.2**. For a narrower crack width, maximum corroded depth not necessarily observed at the un-cracked regions. This can be explained due to the healing of the narrower cracks. For this, corrosion process seems to be stopped or reduced significantly. However, at the un-cracked regions due to the presence of voids at the steel-concrete interface leaded to the formation of deeper pits irrespective of the cement types. A typical case is shown in **Fig. 5.4**. On the other hand, wider cracks are not healed and significant corrosion of the steel bars around the perimeter caused the formation of a bottle-neck as shown in **Fig. 5.5**. Generally, the formation of bottle-neck was clearer over the steel bars in concrete made with blended cements. Further detail investigation separating macro-cell and micro-cell corrosion process of steel bars in concrete is still necessary in order to clarify the exact reason behind this observation. It is clear that in order to enhance long-term durability of concrete structures in the marine environment, the crack widths should be narrower to allow possible healing during its exposure.

5.5 Summary

At the tidal zone, healing of narrower cracks (less than or equal to 0.5 mm) was observed irrespective of the cement types. The depth of corrosion was not necessarily deeper at the cracked region. The presence of voids at the steel concrete interface of the un-cracked region leads the formation of deeper pits. On the other hand, for wider cracks, healing was not observed and steel bars at the cracked region were subjected to significant corrosion. The corrosion of steel bars around the perimeter of the bars caused the formation of bottle-neck. The observation was clearer in the case of slag and fly ash cements compared to ordinary portland cement [15]. Further detail investigation on this matter is still necessary in order to clarify the result.

It is clear from this investigation that to enhance long-term durability, crack widths should be narrow in order to allow healing of the cracks during the exposure. It was also clear that the steel-concrete interface should be free from voids/gaps to ensure long-term durability.

Table 5.2 Pit Depths at the Cracked and Un-cracked Regions

Specimen	Crack Widths (mm) and Pit Depths at Cracked and Un-cracked Regions (mm) *		
	1	2	3
OPC	0.2 (0.5) ((1.0))	0.1 (0.0) ((0.5))	0.1 (0.5) ((1.5))
SCA	0.1 (0.0) ((0.0))	0.3 (0.5) ((1.0))	0.2 (0.0) ((0.0))
SCB	0.3 (0.5) ((0.0))	0.1 (0) ((0.0))	5.0 (3.5**) ((0.0))
SCC	1.5 (1**) ((0.0))	0.1 (0) ((0.0))	2.0 (0.5**) ((0.0))
FACB	0.1 (0.5) ((0.5))	0.3 (1.0) ((0.5))	0.5 (1.5) ((0.5))

*The figures in (.) and ((.)) indicate pit depths at cracked and un-cracked regions respectively. The figures without bracket indicate crack widths. ** Bottle-neck

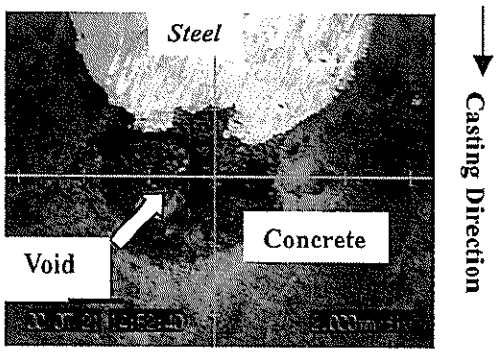

Fig. 5.4 Corrosion at the Un-cracked Region

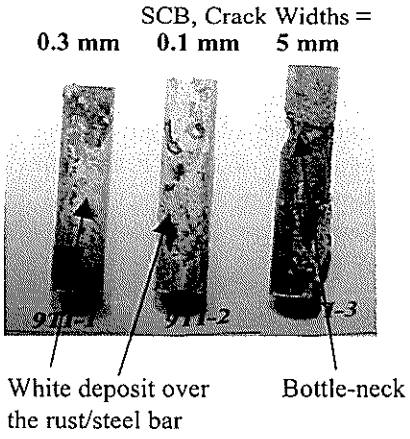

Fig. 5.5 Steel Segments at the Cracked Regions

6. Conclusions

Based on the results of several investigations reported in **Sections 2 ~ 5**, the following conclusions are drawn:

- Voids/gaps at the steel concrete interface cause earlier corrosion and accelerate the corrosion rate.
- Deformed bars are more prone to corrosion compared to plain bars.
- Utilization of slag cement with higher amount of slag, such as slag cement of Type C improves the microstructure of concrete, and reduces the chloride ion ingress in concrete. Corrosion of steel bars in concrete and chloride ion ingress in concrete are sequenced as OPC>FACB>SCA>SCB>SCC.
- With the long-term exposure in the tidal environment, narrower cracks heal irrespective of the cement types.

Acknowledgements

Sincere thanks to the previous members of the *Materials Division, Port and Airport Research Institute, Independent Administrative Institution* for planning of the 23 years, 15 years and 10 years old precious specimens. Some part of this report was carried out at the *Otsuki Laboratory, Department of Civil Engineering, Tokyo Institute of Technology, Japan* during the first author's doctoral study. The authors express their gratitude and sincere thanks to *Prof. Nobuaki Otsuki* for his supervision during the investigations. Thanks are also due to the members of the Otsuki Laboratory for their help during the investigations.

References

1. Malhotra, V. M., Making Concrete "Greener" with Fly Ash, Concrete International, May 1999, pp.61-66.
2. Mohammed, T. U., Otsuki, N., Hisada, M., Corrosion of Steel Bars with Respect to Orientation in Concrete, ACI Materials Journal, Vol. 96, No. 2, March –April 1999, pp.154-159.
3. Mohammed, T.U., Otsuki, N., Hisada, M., and Hamada, H., Marine Durability of 23-Year-Old Reinforced Concrete Beams, Fifth CANMET/ACI International Conference on Durability of Concrete, Barcelona, Spain, ACI SP 192-65, 2000, pp. 1071-1088.
4. Mohammed, T.U., Yamaji, T., Aoyama, T., and Hamada, H., Marine Durability of 15-Year Old Concrete Specimens Made With Ordinary Portland, Slag and Fly Ash Cements, CANMET/ACI International Conference on Fly Ash, Silica Fume and Natural Pozzolans in Concrete, Madras, India, July 22-27, 2001 (accepted).
5. Mohammed, T.U., Otsuki, N., Hamada, H., and Yamaji, T., Chloride Ion Induced Corrosion of Steel Bars in Concrete with the Presence of Gap at the Steel-Concrete Interface (Submitted in ACI Materials Journal).
6. Brown, R.D., Mechanism of Corrosion of Steel in Concrete in Relation to Design, Inspection and Repair of Offshore and Coastal Structures, Performance of Concrete in Marine Environment, ACI SP 65 (1980) 169-204.
7. Otsuki, N., Mohammed, T. U., Hisada, M., Nagataki, S., Corrosion of Plain and Deformed Steel Bars in Cracked Concrete, Fourth CANMET/ACI International Conference on

Recent Advances in Concrete Technology, Supplementary Papers, June 1998, pp.249-268.
8. Mohammed, T.U., Otsuki, N., Hisada, M., and Shibata, T., Effect of Crack Width and Bar Types on Corrosion of Steel in Concrete, Accepted to publish in ASCE Materials Journal.
9. Fontana, M. G., and Greene, N. D., Corrosion Engineering, Second Edition, McGraw-Hill, 1983.
10. Gu, P., Beaudoin, J.J., Zhang, M.H., and Malhotra, V.M., Performance of Reinforcing Steel in Concrete Containing Silica Fume and Blast-Furnace Slag Ponded with Sodium Chloride Solution, ACI Materials Journal, Vol. 97, No. 3, May-June 2000, pp. 254-262.
11. Goto, Y., Cracks Formed in Concrete Around Deformed Tension Bars, Journal of American Concrete Institute, Vol. 68, April 1971, pp.244-251.
12. Arya, C., Ofori-Darko, F. K., Influence of Crack Frequency on Reinforcement Corrosion in Concrete, Cement and Concrete Research, Vol.26, No.3, 1996, pp.345-353.
13. Hansen, E. J. and Saouma, V.E., Numerical Simulation of Reinforced Concrete Deterioration – Part I : Chloride Diffusion, ACI Materials Journal, Vol. 96, No. 2, March-April 1999, pp. 173-180.
14. Nagataki, S., Mineral Admixtures in Concrete : State of the Art and Trends, ACI SP 144, 1993, pp.447-482.
15. Mohammed, T.U., Yamaji, T., Aoyama, T., and Hamada, H., Corrosion of Steel Bar in Cracked Concrete Made With Ordinary Portland, Slag and Fly Ash Cements, CANMET/ACI International Conference on Fly Ash, Silica Fume and Natural Pozzolans in Concrete, Madras, India, July 22-27, 2001 (accepted).
16. Edvardsen, C., Water Permeability and Autogenous Healing of Cracks in Concrete, ACI Materials Journal, Vol. 96, No. 4, July – August 1999, pp. 448-454.